Editors' Suggestion | Featured in Physics

Merged-Beams Study of the Reaction of Cold HD^+ with C Atoms Reveals a Pronounced Intramolecular Kinetic Isotope Effect

Florian Grussie,[1] Lukas Berger,[1] Manfred Grieser,[1] Ábel Kálosi,[2,1] Damian Müll,[1] Oldřich Novotný,[1] Aigars Znotins,[1] Fabrice Dayou,[3] Xavier Urbain,[4] and Holger Kreckel[1,*]

[1]*Max-Planck-Institut für Kernphysik, Saupfercheckweg 1, 69117 Heidelberg, Germany*
[2]*Columbia Astrophysics Laboratory, Columbia University, New York, New York 10027, USA*
[3]*Sorbonne Université, Observatoire de Paris, PSL University, CNRS, LERMA, F-92195 Meudon, France*
[4]*Institute of Condensed Matter and Nanosciences, Université catholique de Louvain, B-1348 Louvain-la-Neuve, Belgium*

(Received 8 December 2023; revised 28 February 2024; accepted 19 March 2024; published 10 June 2024)

We present a merged-beams study of reactions between HD^+ ions, stored in the Cryogenic Storage Ring (CSR), and laser-produced ground-term C atoms. The molecular ions are stored for up to 20 s in the extreme vacuum of the CSR, where they have time to relax radiatively until they reach their vibrational ground state (within 0.5 s of storage) and rotational states with $J \leq 3$ (after 5 s). We combine our experimental studies with quasiclassical trajectory calculations based on two reactive potential energy surfaces. In contrast to previous studies with internally excited H_2^+ and D_2^+ ions, our results reveal a pronounced isotope effect, favoring the production of CH^+ over CD^+ across all collision energies, and a significant increase in the absolute rate coefficient of the reaction. Our experimental results agree well with our theoretical calculations for vibrationally relaxed HD^+ ions in their lowest rotational states.

DOI: 10.1103/PhysRevLett.132.243001

Ion-neutral reactions are important in many fields, ranging from astrophysics and atmospheric chemistry to combustion and industrial applications. In cold interstellar clouds, ion-neutral reactions have been identified as the main drivers for the formation of small molecules in the gas phase [1,2]. Their dominant role in interstellar chemistry is owed to the fact that they can proceed rapidly even at low temperature and low density. In this framework, exothermic processes without a reaction barrier are of particular relevance. Modern interstellar cloud models often contain several thousand rate coefficients for ion-neutral reactions; however, very few of them are based on experimental data. In fact, most of the reaction rates in the models are either sophisticated guesses or extrapolations from measurements conducted at high pressure. The data become even more sparse when deuterated molecules are considered, despite the fact that those molecules are frequently observed in space [3] and used to infer information on important astrophysical parameters. For example, observations of H_2D^+ have been used to derive a minimum age limit for star-forming molecular cores [4]. In these studies, the deuteration can be explained by small differences in zero-point energies [5]. However, while this effect is very important for reactions that are essentially thermoneutral, its relevance for exothermic ion-neutral reactions is less obvious.

Recently, several reactions between sympathetically cooled rare gas ions and ammonia, including fully deuterated ND_3, have been investigated at temperatures between 200 and 300 K. An inverse kinetic isotope effect (where the rate coefficient involving hydrogen-bearing reactants is significantly slower than the rate coefficient for deuterium-bearing reactants $k_H/k_D < 1$) was derived [6,7], indicating a conflict with common capture theories. Measurements in selected-ion flow tubes, however, appear to be at odds with this finding [8], and more research may be needed [9].

At higher collision energies, a number of experiments employing crossed beams [10] and guided ion beam methods [11] with atomic ions have been carried out. Dating back to the 1960s, theoretical models on the isotope effect in strippinglike direct reactions, largely based on classical kinematic and geometric arguments, have been devised. These considerations were used to interpret isotope effects observed in early experiments of atomic ions impinging on hydrogen gas in different isotopic variants [12–17].

A very important but largely unexplored subclass of ion-neutral processes are reactions between neutral atoms and cold molecular ions. For example, many interstellar reaction

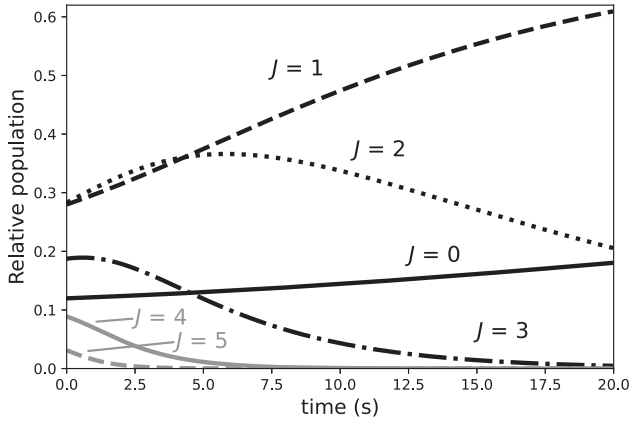

FIG. 1. Evolution of the rotational state populations of HD^+ inside the CSR as a function of time. The model assumes ionization by electron impact at an initial source temperature of 500 K, while the time evolution [25] is based on published Einstein coefficients and level energies [31]. For clarity of presentation, we do not plot levels with $J > 5$, as they have an initial population of $\leq 1\%$.

chains are initiated through reactions between hydrogen molecular ions and neutral atoms, which introduce the heavier species (e.g., carbon and oxygen) into the chemical network and, thus, pave the way for the formation of more complex species. This type of reaction is difficult to study experimentally, as both reactants need to be prepared in specific quantum states for well-defined measurements. While a number of room temperature studies with N and O atoms can be found in the literature [18,19], there are almost no previous reaction studies between cold molecular ions and neutral C atoms, which form the backbone of gas phase organic chemistry in interstellar space. For example, the UMIST database for Astrochemistry [20] lists more than a hundred reactions between molecular ions and neutral C atoms; however, essentially none of the rate coefficients appear to be based on measurements and no energy dependencies are given. Recently, the merged-beams technique has been employed to study collisions of C atoms with H_3^+ [21], H_2^+, and D_2^+ [22] ions, albeit employing rovibrationally excited ions that were extracted directly from standard discharge ion sources. These studies indicated the apparent absence of an intermolecular isotope effect when considering the cross sections between reactions with H_2^+ and D_2^+, while the overall reaction rate coefficients were found to be significantly smaller (by a factor of ~4) than predicted by capture theories [22]. This discrepancy was partly resolved upon examination of the relevant reactive states and the observation that vibrationally excited H_2^+/D_2^+ ions would undergo dissociative charge transfer (see Fig. 7 in [22]).

Here, we present measurements for the reaction

$$HD^+ + C \rightarrow CH^+/CD^+ + D/H \qquad (1)$$

using cold HD^+ ions with the recently commissioned ion-neutral merged-beams collision setup at the Cryogenic Storage Ring (CSR) [23]. The experimental setup has been described in detail elsewhere [24], and more details on the present experiments are given in an accompanying publication [25]; therefore, we will limit ourselves to a brief overview of the measurement principle.

The CSR is a fully electrostatic heavy-ion storage ring with a nested vacuum structure of 35 m circumference. Housed inside a large cryostat, the inner chambers can be cooled to liquid helium temperatures ($T < 5$ K) by a closed-cycle refrigerator. The ion optical lattice allows for the storage of positive or negative ion beams with kinetic energies of up to 300 keV per unit charge, in an extreme vacuum with residual gas number densities on the order of 10^3 particles per cm^3. For technical details on the storage ring layout and performance, see Ref. [23]. Previous studies have shown that diatomic infrared-active molecular ions stored inside the CSR will cool to their lowest rovibrational states by spontaneous emission of radiation [26,27]. This allows for experiments with molecular ions in defined quantum states [28], which greatly simplifies comparison to theoretical calculations.

For the present experiments, HD^+ ions were extracted from a discharge ion source, mass selected by a dipole magnet, and electrostatically accelerated to a kinetic energy of 40 keV. We utilized HD gas inside the source, which is ionized by electron impact. We suppressed the production of triatomic molecular ions by operating the ion source with a minimum amount of gas. To be able to subtract the contribution of a small H_3^+ contamination, we also measured the rate coefficient of vibrationally cold $H_3^+ + C$ forming CH^+ and CH_2^+, as a function of the collision energy (the results are presented in [25]).

After injection, typically 2×10^8 HD^+ ions circulate inside the CSR, where we observe an average beam lifetime of ~15 s. This comparatively fast decay is owed to the small mass of HD^+, making the stored beam susceptible to perturbations by voltage ripple on the electrodes and stray fields, and the large number of ions that were stored at low kinetic energy [23,25].

Inside the cryogenic vacuum of the CSR, the internal excitations of the molecular ions will cool by spontaneous emission of radiation. The vibrational cooling of stored HD^+ ions has been studied *in situ* at the Test Storage Ring, using Coulomb explosion imaging [29]. Those measurements revealed that, after 300 ms of storage, more than 96% of the ions have reached the vibrational ground state. The longest vibrational lifetime is around 60 ms (for the $v = 1$ state), and we expect all ions to have reached the ground vibrational state after ~0.5 s. The rotational cooling is significantly slower but straightforward to predict. Along the lines of previous studies [22,30], we estimate the neutral gas temperature inside the ion source to be 500 K. Assuming that electron impact ionization does not change

the molecular angular momentum, we can infer the initial rotational population of the stored HD^+ ions. It corresponds to a thermal distribution of 245 K, owing to the difference in the rotational constants between HD and HD^+ [25]. The subsequent state evolution is shown in Fig. 1. It can be modeled using published Einstein coefficients and level energies of HD^+ [31]. In the following, we approximate the average rotational population for storage times from 0.5 to 20 s by a thermal distribution with an effective temperature of $T_{\mathrm{eff}} = 150$ K. A more detailed description of the cooling model is given in [25].

During storage, the ions are merged with a neutral C atom beam propagating along one of the straight sections of the CSR. The neutral carbon atoms are produced via photodetachment of a negative C^- beam using a high-power (1.8 kW) diode laser array at a wavelength of 808 nm. The C^- ions are generated inside a cesium sputter ion source and accelerated by an electrostatic platform. On its path toward the CSR, the C^- beam is guided through a dedicated photodetachment chamber, where the laser array neutralizes a fraction of about ~2% of the anions, while the remaining C^- ions are deflected into a Faraday cup. Only C atoms in the ^3P ground term are produced by the photodetachment process. We expect the fine structure sublevels to be occupied statistically [22,32]. The laser (and, thus, the neutral beam) is switched on and off with a period of 6 ms (166 Hz) for background subtraction.

While the energy of the stored ions is kept constant at 40 keV during the experiments, the energy of the neutral beam can be varied to adjust the relative collision energy E_r between the HD^+ and C reactants. In this way, we can perform energy-resolved measurements, which yield a merged-beams rate coefficient $\langle \sigma v_r \rangle$ as a product of the energy-dependent cross section σ and the distribution of the relative velocities v_r (see Appendix A for experimental methods).

Figure 2 shows the measured merged-beams rate coefficients for both reaction channels at storage times from 0.5 to 20 s. For both channels, the data did not reveal any statistically significant changes after 0.5 s. At this time, the ions have reached their vibrational ground state, while the rotational population distribution is still evolving, albeit rather slowly. In fact, inspection of Fig. 1 reveals that the main effect of radiative cooling during this time period is the increase of population in $J = 1$, largely due to the decay of the states with $J = 3$ and $J = 4$. Combined with the fact that only the five lowest rotational states are populated to begin with, this may explain why the rate coefficient of this exothermic reaction remains largely unaffected by the slowly changing rotational populations.

Also shown in Fig. 2 is the rate coefficient for the reaction of D_2^+ with C, which we use to calibrate the absolute scale. The rate coefficients have been corrected for high-energy contributions stemming from the merging and

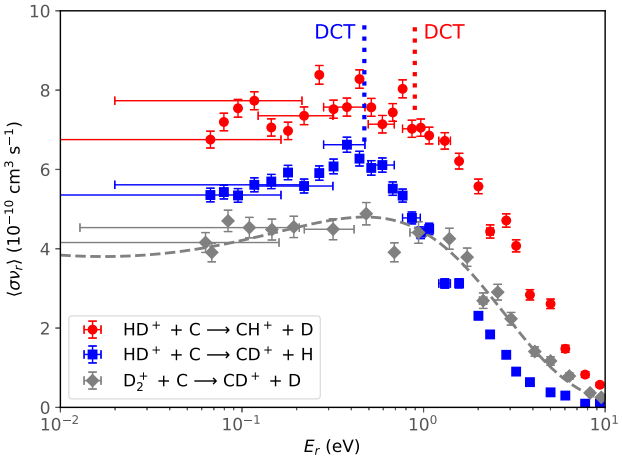

FIG. 2. Merged-beams rate coefficients $\langle \sigma v_r \rangle$ for the reaction of HD^+ with C, as a function of the collision energy E_r. The red and blue markers represent the CH^+ and CD^+ product channels, respectively. Also shown are measurements for the reaction $D_2^+ + C \rightarrow CD^+ + D$, and the corresponding calibration curve, based on previous measurements [22,33]. Note that the data for $D_2^+ + C$ collisions were taken with rovibrationally hot ions, which impacts the overall scale of the rate coefficient. We plot horizontal error bars for a few typical data points. They reflect the width of the simulated collision energy distribution. The vertical error bars reflect the (1σ) counting statistics in each bin, while we assume an additional absolute uncertainty of 20%. The dotted lines indicate the energetic opening of the competing dissociative charge transfer (DCT) reaction, which may differ for both channels according to the pairwise energy model (see the main text and Appendix B).

focusing of the ion beam, using the simulated collision energy distributions [24]. The vertical error bars in the graph represent 1σ uncertainties derived from the counting statistics at each energy. We estimate an additional total uncertainty of ~20% for the absolute scale of the rate coefficients. The lowest energy the experiment can sample in its current form is on the order of 60 meV, limited by the angular divergence of the beams. Details on background subtraction, the data reduction procedure, uncertainties, and the calibration of the absolute rate coefficients are given in an accompanying publication [25].

It is important to note that, since we measure two independent channels for the present reaction, the overall rate coefficient for reactive collisions is represented by the sum of both channels. At low collision energies (≤ 0.1 eV), the total rate coefficient is on the order of $\sim 1.3 \times 10^{-9}$ cm^3 s^{-1}, more than a factor of 3 larger than the rate coefficient for (internally hot) D_2^+ colliding with C and forming CD^+.

The rate coefficients measured for both product channels of reaction (1) provide the cross sections, using $\sigma \simeq \langle \sigma v_r \rangle / \langle v_r \rangle$, where $\langle v_r \rangle$ is the nominal merged-beams value of the relative velocity v_r at the respective setting. The results are shown in Fig. 3 as a function of the relative

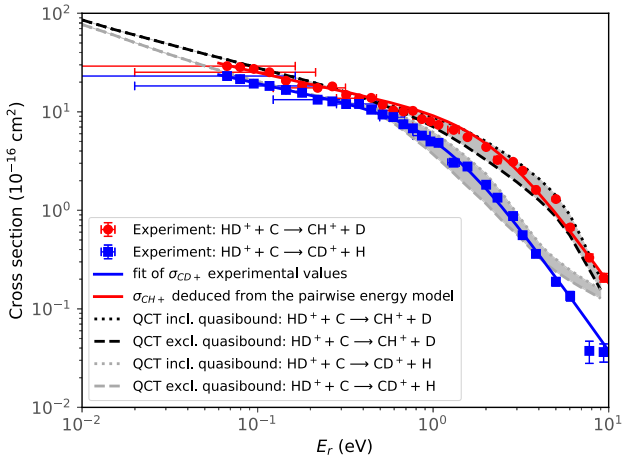

FIG. 3. Reaction cross sections for HD^+ colliding with C as a function of the relative collision energy E_r. The red and blue dots indicate the experimental results for the $CH^+ + D$ and $CD^+ + H$ products, respectively. We plot horizontal error bars for a few typical data points. They reflect the width of the simulated collision energy distribution. For both reaction channels the theoretical (QCT) calculations including and excluding all the product molecules in quasibound states are shown, with the range between these two extreme cases indicated by the shaded areas. Full lines are obtained by fitting $\sigma_{CD^+}(E_r)$ (blue line) and scaling the collision energy according to the pairwise energy model to predict $\sigma_{CH^+}(E_r) \simeq \sigma_{CD^+}(E_r \times \mu_{CH^+}/\mu_{CD^+})$ (red line). The model considers the collision of C with either D^+ or H^+ (see the main text for details).

collision energy E_r. In contrast to previous measurements of the $H_2^+ + C$ and $D_2^+ + C$ reaction cross sections, for which no intermolecular isotope effect was found [22], our measured $HD^+ + C$ reaction cross sections show a pronounced *intramolecular* isotope effect. The CH^+ reaction channel is preferred over the CD^+ channel at all collision energies, and the decline of the cross section at high energies sets in later for CH^+. The decline of both reaction cross sections is attributed to an increasing contribution of the competing dissociative charge transfer (DCT) channel, $HD^+ + C \rightarrow C^+ + H + D$, which is endoergic by 0.46 eV (reduced to 0.34 eV taking into account the HD^+ zero-point energy).

To compare our experimental results to theory, we have carried out dedicated quasiclassical trajectory (QCT) calculations, employing two recently developed *ab initio* potential energy surfaces (PESs), corresponding to the first two electronic states of quartet spin multiplicity, $1^4A'$ and $1^4A''$, of the CH_2^+ system (see Ref. [22] for a discussion of the electronic states that are likely to drive the present reaction and [25] for more details on the QCT calculations). Both the $1^4A'$ and $1^4A''$ states lead to formation of CH^+/CD^+ molecules in the same $^3\Pi$ excited electronic state, corresponding to an exoergicity for reaction (1) of 2.60 eV (reduced to 2.44 and 2.48 eV, taking into account the zero-point energies of CH^+ and CD^+, respectively).

The QCT calculations predict that, above the energy threshold for the DCT channel, a non-negligible fraction of the product molecules are in quasibound states, with enough energy to dissociate but trapped behind a centrifugal barrier. In our experiment, the flight time from the interaction region to the particle detector is on the order of (6 ± 1) μs. As it is difficult to infer the lifetimes of the quasibound states precisely in the calculations, here we have considered two extreme cases. In the first case (including quasibound states) we assume that all of the product CH^+ and CD^+ ions reach the detector, and in the second case (excluding quasibound states) we assume that all molecules in quasibound states will dissociate before they can be detected. The experimental cross sections are compared to the QCT results in Fig. 3. As can be seen, almost across the entire energy range, the agreement between experiment and theory is excellent, indicating that the $1^4A'$ and $1^4A''$ states indeed provide the main contribution to reaction (1). The fact that the experimental cross sections are situated between the two extreme cases considered in the QCT calculations suggests that a fraction (but not all) of the quasibound product molecules reach the detector.

Most remarkably, the theoretical calculations also reproduce the branching ratio of the two possible pathways for reaction (1) almost perfectly (see Fig. 4), except for the highest energy range, where the theoretical branching ratio decreases earlier than the experimental one. This discrepancy, which results from theory overestimating the CD^+ formation (see Fig. 3), may be due to a limited accuracy of

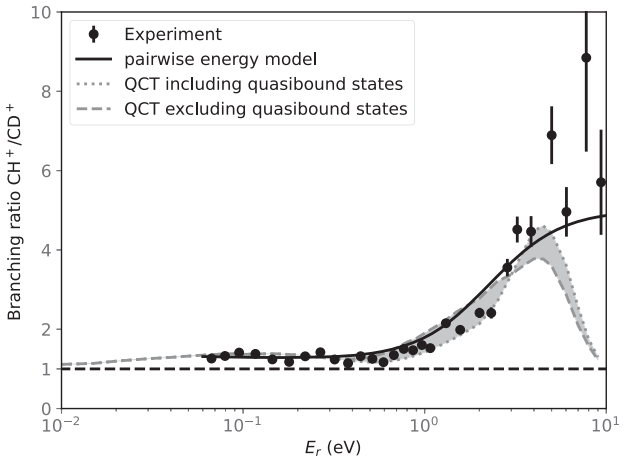

FIG. 4. Measured branching ratio $\sigma_{CH^+}/\sigma_{CD^+}$ of the cross sections of the two pathways for reaction (1) (black dots) compared to the results of QCT calculations (dashed and dotted lines). The shaded area between the two theoretical curves indicates the range between calculations including and excluding all the product molecules in quasibound states, as labeled in the inset. The full line is obtained as the ratio of $\sigma_{CH^+}(E_r) \simeq \sigma_{CD^+}(E_r \times \mu_{CH^+}/\mu_{CD^+})$ and $\sigma_{CD^+}(E_r)$ according to the pairwise energy model (see the main text and Appendix B).

the PESs in the high-energy region. For the exoergic and barrierless ion-neutral reaction studied here, the preference for CH^+ formation over CD^+ can be understood in the following terms. At low collision energies (typically $E_r < 1$ eV), we find a slight preference for the CH^+ channel that is consistent with a higher probability to encounter the H atom at large impact parameters. This effect is driven by the mass asymmetry of the HD^+ molecular ion, for which the center of mass is displaced with respect to the center of charge, causing the opacity function to extend further out for the CH^+ channel compared to CD^+ [34,35]. The marked increase of the branching ratio at higher collision energies ($E_r > 1$ eV) is compatible with the expectations from a strippinglike mechanism of the reaction, where the incident C atom interacts almost exclusively with the H^+ or D^+ ion which is abstracted from HD^+. Stripping models [13,14] state that the cross sections for CH^+ and CD^+ formation are identical when they are compared at the same value of the relative kinetic energy between C and the abstracted atomic ion (this energy is also referred as *pairwise energy* in the literature [36]). Accordingly, the cross section σ_{CD^+} at the collision energy $E_r \times \mu_{CH^+}/\mu_{CD^+}$ can be used to deduce σ_{CH^+} at the collision energy E_r, thereby allowing one to predict the branching ratio $\sigma_{CH^+}/\sigma_{CD^+}$ expected from a stripping mechanism, as described in more detail in Appendix B. As can be seen in Figs. 3 and 4, the results of this model reproduce the measurements for the ratio $\sigma_{CH^+}/\sigma_{CD^+}$ fairly well over almost the entire energy range. Furthermore, the model predicts that the effective energy threshold of the DCT channel depends on whether the H^+ or D^+ ion is abstracted. The predicted values of these threshold energies, indicated in Fig. 2, are consistent with the onset of the decreasing merged-beams rate coefficients.

Note that, based on quantum mechanical considerations, in view of the small difference of the zero-point energy (ZPE) of CH^+ and CD^+, one would expect either no isotope effect (as the ZPEs are very small compared to the total exothermicity) or a preference for the formation of the heavier CD^+ species, contrary to the present findings. In the cold interstellar medium, fundamental reactions with small exothermicities are known to favor the insertion of heavier isotopes [3]. The fact that our studies reveal a small preference of the lighter product instead, owing to kinematic or geometric effects in this barrierless ion-neutral reaction, has great potential significance for isotopic fractionation in the interstellar medium and its quantitative treatment in models involving ion-neutral chemistry. Further studies are foreseen for important interstellar reactions like $H_3^+ + C$ and $H_3^+ + O$, including isotopic variants (H_2D^+ and D_2H^+). Those processes are of paramount importance for the deuterium content of more complex species [3].

This work was supported by the Max Planck Society. The QCT calculations were performed using HPC resources from GENCI-IDRIS (Grant No. 2023-100538). F. G. and H. K. were supported by the European Research Council under Grant Agreement No. StG 307163. X. U. is a Senior Research Associate of the Fonds de la Recherche Scientifique—FNRS and acknowledges support under Grant No. 4.4504.10.

Appendix A: Experimental methods.—The photodetachment of the C^- beam takes place inside a voltage drift tube, allowing us to tune the relative energy of the neutral C atoms with respect to the stored ions. For each injection cycle, we set the drift tube voltage to a fixed value between -1 and $+5$ kV, translating into nominal ion-neutral collision energies between 0 and 10 eV in the center-of-mass reference frame. The C atom beam is collimated by two 4.5 mm apertures separated by 2.9 m in the injection beam line and propagates ballistically thereafter. After traversing the interaction zone inside the CSR, the neutrals are collected in a dedicated cup [24], where the neutral flux can be monitored continuously by secondary electron emission.

The reaction products are guided into an extraction beam line [24], where they are separated from the neutral beam by electrostatic fields, mass selected by a set of two 55° deflectors, and eventually recorded as individual particle events by a channel electron multiplier (CEM). The background-subtracted product count rate S is typically smaller than $10\ s^{-1}$, and the CEM has a near-unity detection efficiency at the energies used here.

Our measurements yield a merged-beams rate coefficient as a product of the energy-dependent cross section σ and the distribution of the relative velocities v_r. It is given by

$$\langle \sigma v_r \rangle = \frac{S}{T_p \eta} \frac{e^2}{I_C I_{HD^+}} \frac{v_C v_{HD^+}}{L \langle \Omega(z) \rangle}, \tag{A1}$$

where S denotes the count rate of the reaction product (CH^+ or CD^+); T_p represents the product transmission of the extraction beam line; e stands for the unit charge; η denotes the detection efficiency of the CEM; v_C and v_{HD^+} represent the velocities of the C atoms and the HD^+ ions, respectively; and $L\langle \Omega(z) \rangle$ denotes the product of the length of the interaction section L and the averaged overlap form factor $\langle \Omega(z) \rangle$ along the interaction region (see Ref. [24] for details). The current attributed to the circulating ions is given by I_{HD^+}. As in previous merged-beams studies [21,24,37–39], we artificially attribute one elementary charge to each neutral atom and treat the neutral flux as a current I_C.

To evaluate $\langle \sigma v_r \rangle$, we need to record all the parameters on the right-hand side of Eq. (A1). The largest uncertainty in this framework is the determination of the overlap factor $\Omega(z)$ [24]. While the neutral beam profile is straightforward to evaluate, the profile of the stored ion beam can only be inferred from time-consuming imaging studies,

determining the emittance of the beam and its evolution along the overlap region. In the present study, we therefore make use of the fact that the particle trajectories inside the electrostatic ion optical lattice of the CSR—and, thus, the ion beam profile—are independent of the particle mass. In particular, at large numbers of stored ions, we find that the emittance of the stored beam depends almost exclusively on the number of ions in the ring. We make use of this fact by linking our data to previous benchmark measurements of the reaction of $D_2^+ + C \rightarrow CD^+ + D$ [22,24]. To this end, we have performed an independent measurement of the above reaction during the same experimental campaign, using identical storage ring settings. Details on the absolute calibration of the merged-beams results are given in an accompanying publication [25].

Appendix B: Pairwise energy model.—Both measurements and QCT calculations for the $HD^+ + C$ reaction show an intramolecular isotope effect in favor of the production of CH^+ over CD^+. More specifically, the ratio of the partial rate coefficients k_{CH^+}/k_{CD^+} exceeds unity at all collision energies. The ratio varies slightly between 1.2 and 1.4 below 1 eV and rises steeply at higher energies (see Fig. 4). Similar intramolecular isotope effects have been observed previously in ion-neutral reactions involving HD or HD^+ species [11,13,40].

At high energy (above 1 eV), the $HD^+ + C$ reaction is believed to proceed via a direct stripping mechanism where C interacts almost exclusively with the H^+ or D^+ that is picked up from HD^+, leaving the other atom almost unaffected. In the so-called pairwise energy model [36,40], one expects that the reaction cross sections for CH^+/CD^+ formation depend on the relative (also called pairwise) kinetic energies between C and the abstracted atom (H^+ or D^+):

$$E_{CH^+} = \frac{1}{2}\mu_{CH^+} v_r^2, \tag{B1}$$

$$E_{CD^+} = \frac{1}{2}\mu_{CD^+} v_r^2, \tag{B2}$$

where v_r is the relative velocity between C and the abstracted atom. Assuming that v_r also corresponds to the relative velocity between C and HD^+, the collision energy writes as

$$E_r = \frac{1}{2}\mu_{C,HD^+} v_r^2, \tag{B3}$$

and the pairwise kinetic energies relate to E_r as

$$E_{CH^+} = \frac{\mu_{CH^+}}{\mu_{C,HD^+}} E_r \simeq 0.38 E_r, \tag{B4}$$

$$E_{CD^+} = \frac{\mu_{CD^+}}{\mu_{C,HD^+}} E_r \simeq 0.72 E_r. \tag{B5}$$

If the reaction probability is primarily governed by the requirement to overcome the centrifugal potential, then, in the case of a stripping mechanism, we have to consider the effective potential between C and the abstracted atom:

$$V^{\text{eff}}_{CH^+} = \frac{E_{CH^+} b^2}{r^2} + V(r), \tag{B6}$$

$$V^{\text{eff}}_{CD^+} = \frac{E_{CD^+} b^2}{r^2} + V(r), \tag{B7}$$

where b is the impact parameter and r is the internuclear distance. Since the interaction potentials $V(r)$ between C and H^+, and between C and D^+, are identical, the centrifugal potentials $V^{\text{eff}}_{CH^+}$ and $V^{\text{eff}}_{CD^+}$ are also identical for given values of the pairwise energy and impact parameter. In such a case, the reaction cross sections σ_{CH^+} and σ_{CD^+} are expected to be identical when they are compared at the same pairwise energy. Accordingly, using Eqs. (B4) and (B5), the two reaction cross sections should relate as follows:

$$\sigma_{CH^+}(E_r) \simeq \sigma_{CD^+}\left(\frac{\mu_{CH^+}}{\mu_{CD^+}} E_r\right) \simeq \sigma_{CD^+}(0.53 \times E_r). \tag{B8}$$

This proportionality is satisfactorily verified for the present reaction by fitting one of the cross sections and scaling it for comparison with the other, as illustrated in Fig. 3.

Above the energy threshold for the dissociative charge transfer (DCT) reaction,

$$HD^+ + C \rightarrow C^+ + H + D, \tag{B9}$$

the pairwise energy model should still be valid if the H and D departing atoms are equally effective in carrying away a given amount of excess energy to form a stable CH^+ or CD^+ product molecule. If it is indeed the case, Eq. (B8) tells us that the cross sections σ_{CH^+} and σ_{CD^+} will start to fall off at collision energies which differ by about a factor of 2. Applying Eqs. (B4) and (B5) with pairwise energies equal to the DCT threshold of 0.34 eV, one predicts the partial cross sections for CH^+ and CD^+ formation to decrease for collision energies above 0.89 and 0.47 eV, respectively. These effective threshold energies, which match the global trend of the measured rate coefficients, are indicated with vertical dotted lines in Fig. 2.

*holger.kreckel@mpi-hd.mpg.de

[1] W. D. Watson, Astrophys. J. **183**, L17 (1973).
[2] E. Herbst and W. Klemperer, Astrophys. J. **185**, 505 (1973).
[3] T. J. Millar, Astron. Geophys. **46**, 2.29 (2005).
[4] S. Brünken, O. Sipilä, E. T. Chambers, J. Harju, P. Caselli, O. Asvany, C. E. Honingh, T. Kamiński, K. M. Menten, J. Stutzki, and S. Schlemmer, Nature (London) **516**, 219 (2014).

[5] E. Hugo, O. Asvany, and S. Schlemmer, J. Chem. Phys. **130**, 164302 (2009).
[6] L. S. Petralia, A. Tsikritea, J. Loreau, T. P. Softley, and B. R. Heazlewood, Nat. Commun. **11**, 173 (2020).
[7] A. Tsikritea, K. Park, P. Bertier, J. Loreau, T. P. Softley, and B. R. Heazlewood, Chem. Sci. **12**, 10005 (2021).
[8] S. G. Ard, A. A. Viggiano, B. C. Sweeny, B. Long, and N. S. Shuman, Nat. Commun. **13**, 3310 (2022).
[9] L. S. Petralia, A. Tsikritea, J. Loreau, T. P. Softley, and B. R. Heazlewood, Nat. Commun. **13**, 3311 (2022).
[10] P. M. Hierl, Z. Herman, and R. Wolfgang, J. Chem. Phys. **53**, 660 (1970).
[11] J. D. Burley, K. M. Ervin, and P. B. Armentrout, Int. J. Mass Spectrom. Ion Process. **80**, 153 (1987).
[12] K. Lacmann and A. Henglein, Ber. Bunsenges. Phys. Chem. **69**, 286 (1965).
[13] A. Henglein, K. Lacmann, and B. Knoll, J. Chem. Phys. **43**, 1048 (1965).
[14] A. Henglein, in *Ion-Molecule Reactions in the Gas Phase*, edited by P. J. Ausloos (American Chemical Society, Washington, DC, 1966), p. 63.
[15] M. A. Berta, B. Y. Ellis, and W. S. Koski, in *Ion-Molecule Reactions in the Gas Phase*, edited by P. J. Ausloos (American Chemical Society, Washington, DC, 1966), p. 80.
[16] L. Friedman, in *Ion-Molecule Reactions in the Gas Phase*, edited by P. J. Ausloos (American Chemical Society, Washington, DC, 1966), p. 87.
[17] J. H. Futrell and F. P. Abrahamson, in *Ion-Molecule Reactions in the Gas Phase*, edited by P. J. Ausloos (American Chemical Society, Washington, DC, 1966), p. 107.
[18] M. Sablier and C. Rolando, Mass Spectrom. Rev. **12**, 285 (1993).
[19] T. P. Snow and V. M. Bierbaum, Annu. Rev. Anal. Chem. **1**, 229 (2008).
[20] D. McElroy, C. Walsh, A. J. Markwick, M. A. Cordiner, K. Smith, and T. J. Millar, Astron. Astrophys. **550**, A36 (2013).
[21] A. P. O'Connor, X. Urbain, J. Stützel, K. A. Miller, N. de Ruette, M. Garrido, and D. W. Savin, Astrophys. J. Suppl. Ser. **219**, 6 (2015).
[22] P.-M. Hillenbrand, K. P. Bowen, F. Dayou, K. A. Miller, N. de Ruette, X. Urbain, and D. W. Savin, Phys. Chem. Chem. Phys. **22**, 27364 (2020).
[23] R. von Hahn *et al.*, Rev. Sci. Instrum. **87**, 063115 (2016).
[24] F. Grussie, A. P. O'Connor, M. Grieser, D. Muell, A. Znotins, X. Urbain, and H. Kreckel, Rev. Sci. Instrum. **93**, 053305 (2022).
[25] See the companion paper, F. Grussie, L. Berger, M. Grieser, Á. Kálosi, D. Müll, O. Novotný, A. Znotins, F. Dayou, X. Urbain, and H. Kreckel, Phys. Rev. A **109**, 062804 (2024); for details on the subtraction of the H_3^+ contamination, the normalization of the rate coefficient of the $HD^+ + C$ reaction, and absolute uncertainties for the rate coefficient measurements.
[26] A. P. O'Connor *et al.*, Phys. Rev. Lett. **116**, 113002 (2016).
[27] C. Meyer *et al.*, Phys. Rev. Lett. **119**, 023202 (2017).
[28] O. Novotný *et al.*, Science **365**, 676 (2019).
[29] Z. Amitay, A. Baer, M. Dahan, L. Knoll, M. Lange, J. Levin, I. F. Schneider, D. Schwalm, A. Suzor-Weiner, Z. Vager, R. Wester, A. Wolf, and D. Zajfman, Science **281**, 75 (1998).
[30] F. von Busch and G. H. Dunn, Phys. Rev. A **5**, 1726 (1972).
[31] C. M. Coppola, L. Lodi, and J. Tennyson, Mon. Not. R. Astron. Soc. **415**, 487 (2011).
[32] M. Scheer, R. C. Bilodeau, C. A. Brodie, and H. K. Haugen, Phys. Rev. A **58**, 2844 (1998).
[33] G. F. Schuette and W. R. Gentry, J. Chem. Phys. **78**, 1777 (1983).
[34] J. C. Light and S. Chan, J. Chem. Phys. **51**, 1008 (1969).
[35] P. M. Hierl, J. Chem. Phys. **67**, 4665 (1977).
[36] J.-B. Song and E. A. Gislason, Chem. Phys. **212**, 259 (1996).
[37] H. Kreckel, H. Bruhns, M. Čížek, S. C. O. Glover, K. A. Miller, X. Urbain, and D. W. Savin, Science **329**, 69 (2010).
[38] K. A. Miller, H. Bruhns, J. Eliášek, M. Čížek, H. Kreckel, X. Urbain, and D. W. Savin, Phys. Rev. A **84**, 052709 (2011).
[39] K. A. Miller, H. Bruhns, M. Čížek, J. Eliášek, R. Cabrera-Trujillo, H. Kreckel, A. P. O'Connor, X. Urbain, and D. W. Savin, Phys. Rev. A **86**, 032714 (2012).
[40] W. R. Gentry, E. A. Gislason, B. H. Mahan, and C. Tsao, J. Chem. Phys. **49**, 3058 (1968).